AIP | Review of Scientific Instruments

Note: Advancement in tip etching for preparation of tunable size scanning tunneling microscopy tips

J. P. Corbett, S. G. Pandya, A.-O. Mandru, J. Pak, M. E. Kordesch, and A. R. Smith

Citation: Review of Scientific Instruments **86**, 026104 (2015); doi: 10.1063/1.4907706
View online: http://dx.doi.org/10.1063/1.4907706
View Table of Contents: http://scitation.aip.org/content/aip/journal/rsi/86/2?ver=pdfcov
Published by the AIP Publishing

Note: Advancement in tip etching for preparation of tunable size scanning tunneling microscopy tips

J. P. Corbett, S. G. Pandya, A.-O. Mandru, J. Pak, M. E. Kordesch, and A. R. Smith[a)]
Department of Physics and Astronomy, Nanoscale and Quantum Phenomena Institute, Ohio University, Athens, Ohio 45701, USA

(Received 3 September 2014; accepted 26 January 2015; published online 12 February 2015)

The two aspects of a scanning tunneling microscopy tip, the macroscopic profile and the nanoscale apex, can be tailored by controlling the tension during electrochemical etching and the solution-electrode contact area via acetone vapor. The apex diameter is shown to be proportional to the square root of the tension, and is demonstrated over apex diameters of 150-500 nm. The apex was found to be created in four distinct shapes where a secondary etching can reshape the tip into a single geometry. Improvement in tip height and stability of the profile are demonstrated versus a non-acetone fabrication control. © *2015 AIP Publishing LLC.* [http://dx.doi.org/10.1063/1.4907706]

The scanning tunneling microscopy (STM) tip plays a key role in acquiring high quality STM images;[1] however, since there is no one tip that can perform all the robust techniques (e.g., spectroscopy, spin-polarized) that STM can achieve, different types of tips are needed for different applications. Building on the decades of tip fabrication research (which focused on creating and controlling ultra-sharp STM tips[2–4]), this work strives to understand further the art and science of tip creation, and how to tailor tips which can be taken further for different applications.

In the experiment, a 200 ml, 2M NaOH solution is used to electrochemically etch a 3N8 purity, 0.020″ diameter, W wire under a 4.0 V AC potential applied between the W wire (primary electrode) and a carbon counter-electrode.[5,6] A specially designed C-flex bobber sheaths the wire, providing insulation from the solution and restricting the reaction to occur at the air-solution-electrode (ASE) interface [see Figs. 1(a) and 1(b)]. The tip is formed from the necked region where the tip shaft fractures from the primary electrode and drops off. The bobber additionally provides buoyancy to control the tension [see Fig. 1(a)]. The bobber is made of 4 components, two layers of C-flex tubing and two Viton O-rings [see Fig. 1(a)]. The C-flex sheath has a specific gravity of 0.90 making it buoyant in the 1.08 specific gravity NaOH solution. The Viton O-ring has a specific gravity of 1.60 making it heavier than the solution but is necessary to hold the bobber together due to a mismatch in inner (ID) and outer (OD) diameters of the two layers of tubing.

An additional 0.75 ml of acetone is added to the solution to assist in limiting the W electrode's exposure to the solution surface.[7] This small addition of acetone does not homogeneously mix with the entire solution but rather forms a very thin (approximately 11 microns thick) acetone layer atop of the NaOH solution. The thin acetone layer alters the surface hydrodynamics by facilitating a radial movement of H_2 gas bubbles away from the W electrode. If the acetone layer becomes too thick (about 70 microns, or roughly 5 ml of acetone), the ASE interface becomes an air-acetone-electrode interface thereby terminating the etching.

The acetone vapor is the key element in reducing the solution-electrode contact area. A pipette modified to release acetone vapor from an absorbent tip with a liquid acetone reservoir is mounted a few mm from the ASE interface. The acetone vapor saturates the ASE interface reducing the contact area during etching by limiting the size of the H_2 gas bubbles [see Fig. 1(c)]; the acetone layer then assists in removing the reduced size bubbles from the W electrode with an end result of a reduction in solution to W contact area.

The solution to electrode contact determines the tip profile which has two features that affect tip performance: the aspect ratio (the ratio of tip height to wire diameter) and the mechanical stability (i.e., the geometry of the tip profile)[8] [see Figs. 2(a)–2(c)]. To quantify the mechanical stability of the tip, a radius of curvature along the edge of the profile (PROC) is measured, using scanning electron microscopy (SEM), and normalized to the height of the tip, which allows for comparison between tips of varying lengths [see Fig. 2(c)].

The etching undergoes three stages [see Figs. 1(b)–1(d)]: an initial alignment stage to the solution surface, a first reduction in the ring of H_2 bubbles that move radially away from the W electrode, and a second final bubble ring reduction that constricts the etching to the ID of the bobber. To investigate the effect of the acetone, two controls were utilized: (1) tips made with no acetone and (2) tips with acetone but only with a first bubble ring reduction. The tips created with a second bubble ring reduction see an improvement in both stability (with a higher normalized PROC) and lower aspect ratio [see Fig. 2(e)].

The reaction etches a necked region out of the primary electrode where the tip shaft detaches under the weight of the bobber once the system exceeds the tensile strength of the W forming the STM tip.[9] The tip that is formed has three features that determine its functionality: the apex diameter, the terminating radius of curvature (TROC), and the apex shape [see Figs. 3(a)–3(d)]. This necking region experiences a tension that is considered to be quasi-static and is a func-

a)Author to whom correspondence should be addressed. Electronic mail: smitha2@ohio.edu

tion of the weight downward and the buoyancy upward [see Fig. 1(a)]. Knowing the specific gravity and the weight of each component of the system, the buoyancy is determined by the ratio of weight:specific gravity.[10] With the buoyancy known, the tension is determined using Newton's second law and rearranging for the tension, one gets in the end:

$$T = \frac{g[m_C S_W S_O (S_C - 1) + m_W S_O S_C (S_W - 1) + m_O S_C S_W (S_O - 1)]}{S_C S_W S_O}, \tag{1}$$

where T is the tension, and m, S, and g are the mass, specific gravity, and gravitational acceleration, respectively; subscripts C, O, and, W are indicators for C-flex, O-ring, and tungsten, respectively. The error on the tension is determined to a 1.5 dyne precision. This is likely an underestimation in the error of the tension due to external factors like bubbling from the reaction and floor vibrations, which have been shown to affect tip size.[11]

To characterize the effect of tension on the apex diameter during etching, tips are fabricated in data sets of 5-10 tips for a particular tension. The apex diameter of each tip is measured using SEM, and an average apex diameter and standard deviation over the data set are calculated. Several data sets are produced at different tensions and a plot of average apex diameter versus tension is shown in Fig. 3(e). A trend appears in the average apex diameter versus tension data in Fig. 3(e). To model this behavior, the apex is considered to be a uniform cylinder with an applied tension T along the axial direction. By knowing the tension from Eq. (1) and the physical properties of tungsten, the apex diameter (D) that the wire fractures at can be theoretically estimated from the ultimate tensile strength (U) given by the equation:

$$D = 2\sqrt{\frac{T}{\pi U}}. \tag{2}$$

A suitable choice of U must be made for use in Eq. (2). It is know that the U of W increases as the diameter (d) of the wire

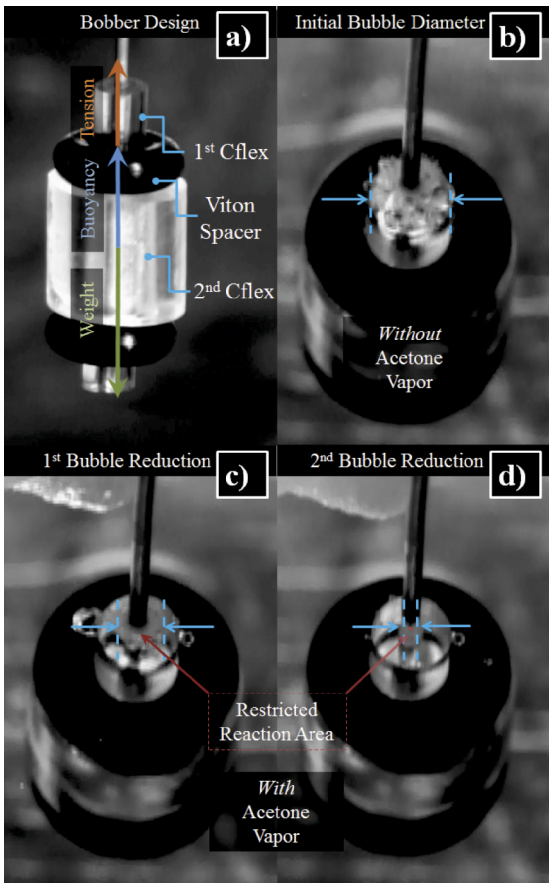

FIG. 1. Photographs of the bobber. (a) Side view of the bobber overlaid with a free body diagram, with blue indicators making the design elements of the bobber. (b)–(d) images show a downward angle of (a), indicating the 3 stage progression of bubble ring reduction during etching. The red arrows indicate the area the reaction is restricted to on the W electrode.

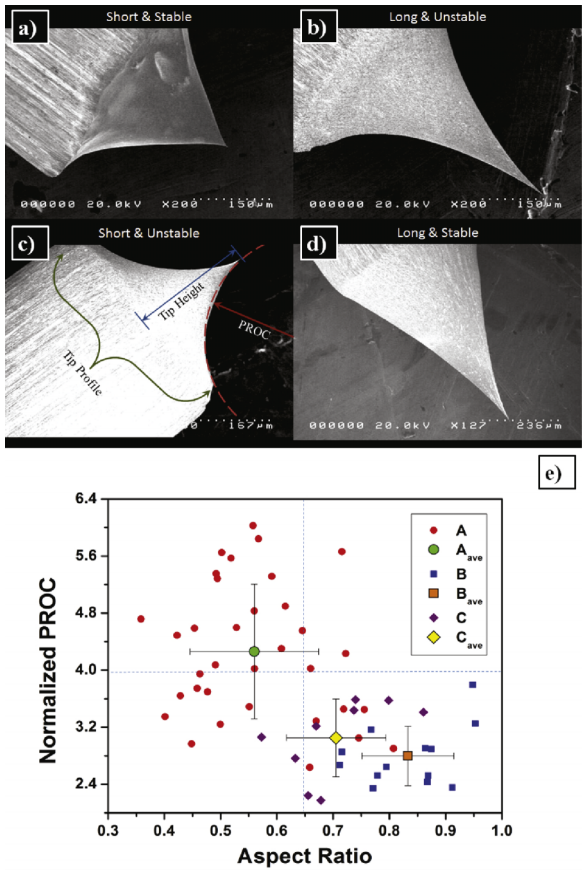

FIG. 2. SEM images of the tip profile with accompanying data. (a)–(d) show four combinations of tip height and stability, with (c) additionally defining the PROC, tip height, and tip profile. (e) plots the experimental data of reducing the ASE interface. Set A is data with a second bubble ring reduction, set B is data with the first bubble ring reduction, and C is data without acetone, where the subscript "ave" specifies average.

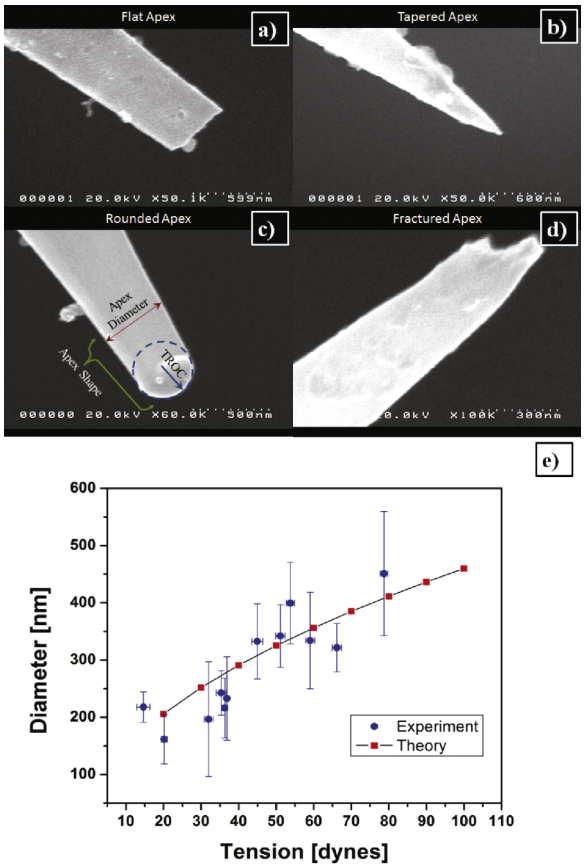

FIG. 3. SEM images of the tip apex with accompanying data. (a)–(d) show the four possible apex shapes, with (c) additionally defining the apex diameter, the TROC, and the apex shape. (e) Comparison between the experimental and theoretical data for average apex diameter versus tension.

decreases.[12] The polycrystalline W wire used in the present work is fabricated by compacting and sintering W granules forming a composite of many long granular micro-wires that collectively make the total wire. Initially, a 0.020″ diameter wire is etched to the diameter of one micro-wire. Therefore, the U that should be chosen, is not from a composite of many granules, but the U for a singular micro-wire diameter, which has a U of 514.04 MPa.

Now with an appropriate U and varying T in Eq. (2), a theoretical estimate of the apex diameter can be produced, and this is plotted in Fig. 3(e) as the solid curve. The theoretical estimate is in agreement with the experimental data. Thereby knowing the tension on the system and U of the material, a tip can be fabricated to a specific diameter. This gives an upper limit to the TROC used for scanning, where the TROC is less than D/2. By minimizing the tension during etching, a very small TROC can be produced for ultrasharp tips with a usability up to 80%.

The apex shape that forms on the tip by detaching from the primary electrode is categorized into four distinct apex geometries: flat, tapered, fractured, and round [see Figs. 3(a)–3(d)]. Each shape occurs with a given probability: flat tips happen about 7% of the time, tapered tips 25%, fractured tips 35%, and round tips happen 33%. Some researchers show very sharp tips and state reproducibility of their tip creation method, but few claim percentages of reproducibility or any variation in the apex shape other than sharp.

With the variety of tip shapes, a secondary, polish etching procedure similar to the one demonstrated by A. H. Sorensen *et al.*, is utilized.[13] The tip is reinserted pointing downward into a second 2M NaOH solution with a 2.0 V potential and polished for approximately 250 ms. All tips that were given a polish resulted in a single rounded geometry with 100% occurrence with an average TROC = 122 nm ± 38 nm. The second polish etching has the possibility to reshape all tips to high quality round tips, regardless of initial apex shape, up to 100% reproducibility, although the second polish results in a round tip with a larger TROC than initial TROC formed by the low tension drop off method. For spectroscopy or spin-polarized STM measurements, a round tip may be preferable, and this second polishing method is suitable for the creation of these tips.

To conclude, it is demonstrated that when restricting the reaction area on the W electrode with acetone vapor a short and mechanically stable tip is produced. Additionally, it is shown that the tip apex diameter depends on the square root of the tension applied during etching. When the tip detaches from the primary electrode, after etching is complete, the apex can terminate into one of four distinct shapes: flat, tapered, fractured, and round. A secondary 2M and 2.0 V AC etching is able to reshape the apex into a single, rounded shape with a TROC = 122 ± 38 nm.

Research supported by the U.S. Department of Energy, Office of Basic Energy Sciences, Division of Materials Sciences and Engineering under Award No. DE-FG02-06ER46 317 (J.P.C.), by the Condensed Matter and Surface Science Program at Ohio University (S.G.P.), and by the U.S. National Science Foundation under Award No. DMR-1206636 (A.O.M. and J.P.). Authors also thank Mr. Doug Shafer for helpful discussions.

[1]E. J. Snyder, E. A. Eklund, and R. S. Williams, Surf. Sci. **239**, L487–L492 (1990).
[2]A. J. Melmed, J. Vac. Sci. Technol., B: Microelectron. Nanometer Struct. **9**, 601 (1991).
[3]P. Kim, J. H. Kim, M. S. Jeong, D. Ko, J. Lee, and S. Jeong, Rev. Sci. Instrum. **77**, 103706 (2006).
[4]W. T. Chang, I. S. Hwang, M. T. Chang, C. Y. Lin, W. H. Hsu, and J. L. Hou, Rev. Sci. Instrum. **83**, 083704 (2012).
[5]A.-S. Lucier, M.S. thesis, McGill University, 2004.
[6]R. Stone, M. Rosamond, K. Coleman, M. Petty, O. Kolosov, L. Bowen, V. Dubrovskii, and D. ZeZe, Rev. Sci. Instrum. **84**, 035107 (2013).
[7]L. Libioulle, Y. Houbion, and J. Gilles, Rev. Sci. Instrum. **66**, 97 (1995).
[8]G. B. Basnet, J. K. Schoelz, P. Xu, S. D. Barber, M. L. Ackerman, and P. M. Thibado, J. Vac. Sci. Technol., B: Microelectron. Nanometer Struct. **31**, 043201 (2013).
[9]S. Kerfriden, A. H. Nahle, S. A. Campbell, F. C. Walsh, and J. R. Smiths, Electrochim. Acta **43**(12-13), 1939-1944 (1998).
[10]P. Tipler and G. Mosca, *Physics for Scientist and Engineers*, 5th ed. (W. H. Freeman, 2003).
[11]Gh. Tahmasebipour, Y. Hojjat, V. Ahmadi, and A. Abdullah, Scanning **31**, 65–74 (2009).
[12]F. F. Schmidt and H. R. Ogden, *The Engineering Properties of Tungsten and Tungsten Alloys Volume 191 of Report (Defense Metals Information Center)* (Battelle Memorial Institute, Defense Materials Information Center, 1963).
[13]A. H. Sorensen, U. Hvid, M. W. Mortensen, and K. A. Mørch, Rev. Sci. Instrum. **70**, 3059 (1999).